Journal of Fluids and Structures (2000) **14,** 65–85
doi:10.10061/jfls. 1999.0255, available online at http://www.idealibrary.com on IDEAL®

VORTEX-EXCITED VIBRATIONS OF UNIFORM PIVOTED CYLINDERS IN UNIFORM AND SHEAR FLOW

S. Balasubramanian, and R. A. Skop

Division of Applied Marine Physics, Rosenstiel School of Marine and Atmospheric Science, University of Miami, Miami, FL 33149, U.S.A.

AND

F. L. Haan Jr and A. A. Szewczyk

Department of Aerospace and Mechanical Engineering, University of Notre Dame, Notre Dame, IN 46556, U.S.A.

(Received 23 April 1998 and in final form 15 July 1999)

The vortex-excited dynamics of a uniform pivoted cylinder in uniform and sheared flow was investigated experimentally. The experiments were numerically simulated using a diffusive Van der Pol oscillator model developed by Balasubramanian & Skop recently. Salient features of the experimental investigations and the numerical simulations are presented here. Comparisons between the experimentally recorded and numerically predicted structural response to vortex-excited vibrations, power spectral density measurements of near-wake velocity fluctuations and lock-in ranges are made. A comparison of the numerical predictions and the experimental data reveals good agreement.

1. INTRODUCTION

Separation of flow behind a bluff body leads to fluctuating lift and drag forces. These oscillatory forces can result in substantial body motion if the structure is flexible or elastically restrained. The amplification of these forces due to resonance between the vortex shedding frequency or one of its subharmonics and a body natural frequency is a serious problem in many engineering applications. Termed lock-in or synchronization, this phenomenon has been the focus of decades of research. While a resonance between the vortex-shedding frequency and a body frequency is not in itself surprising, the fact that a resonant structural response is observed over a bandwidth of 25–30% (Sarpkaya 1978) of the resonant frequency makes it significant. The nature of the response close to the linear resonance condition is indicative of nonlinear interaction between the structure and the fluid flow.

Over the years, numerous experimental and numerical investigations have been conducted to understand the dynamics of vortex shedding during lock-in and the dynamics of the cylinder under lock-in. The results of these investigations reveal that the structural response to vortex excitation is primarily governed by a parameter termed the reduced damping. Reduced damping is defined as the structural damping divided by the ratio of fluid to structural masses. Experimental investigations by several investigators have revealed that the structural response to vortex excitation approaches an asymptotic limit of about two

0889–9746/00/010065 + 21 $35.00/0

cylinder diameters for small values of the reduced damping. Numerical investigations using nonlinear oscillator models have identified a modal scaling principle for the structural response. This modal scaling principle (Griffin 1982) collapses the vortex-excited response of different types of structures to a single curve through a modal shape factor.

Nonlinear wake oscillator models have been used to model vortex-excited vibrations of structures for about two decades now. In these equations, the lift force due to vortex shedding is represented by a nonlinear differential equation. Initially, their use was justified by the similarities between the experimental observations of the near-wake velocity fluctuations and the nature of the solutions to these nonlinear oscillators. More recently, a more physical rationale for their use has been provided by the findings of Alberéde & Monkewitz (1992), who showed that nonlinear oscillators of the Van der Pol type arise as a leading-order approximation to the vortex-shedding instability from a uniform stationary cylinder in a uniform flow. This leading-order nature explains the success of the nonlinear oscillator models in matching experimentally observed response amplitudes and the flow velocities at which they occur, while at the same time offering an explanation for their inherent limitations. Recently, Skop & Balasubramanian (1997) have overcome a long-standing limitation of the nonlinear oscillator models, namely, their inability to match the experimentally observed asymptotic limit on the structural response. Skop & Balasubramanian (1997) have introduced a stall-type term in the representation of the fluctuating lift force due to vortex shedding. In their model, they describe the excitation component of the fluctuating lift force that drives cylinder motion by a Van der Pol oscillator. The other component of the lift force is given by a stall term that provides for a self-limiting asymptotic response at zero structural damping.

While vortex-excited vibrations of uniform cylinders in uniform flow have been studied comprehensively over the years, very little attention has been paid to the effect of shear in the approach flow on vortex-excited vibrations. Vortex-excited vibration in nonuniform flow is an oft-experienced phenomenon in marine environments, where depth-varying ocean currents are very common and affect the performance of drill pipe risers and oceanographic moorings. Over land, atmospheric boundary layers and wind shear can result in spanwise-varying fluid loading on smoke stacks and chemical plant towers (Goyder 1997). Shear in the flow results in a variation of the vortex-shedding frequency along the span of the cylinder. Experimental evidence of vortex shedding from rigid cylinders in shear flow indicate that vortices are shed in cells of constant frequency along the span (Stansby 1976). In a nonuniform flow scenario, some part of a flexible cylinder may be under lock-in over a larger range of flow velocities than in uniform flow. Fischer *et al.* (1980) have reported that shear in the flow does not have any significant effect on the observed structural response. Chung (1987) and Kim *et al.* (1984) have reported on the response of tensioned cables to vortex shedding in sheared flows. While Chung (1987) does not present any quantitative evidence of the effect of shear, he suggests that caution must be employed in extrapolating the uniform flow data to nonuniform flow scenarios. Kim *et al.* (1985) report multi-moded nonlock-in behavior in shear flows. More recently, Vandiver *et al.* (1996) have reported the existence of regimes of lock-in and nonlock-in response in highly sheared flows. Research into vortex-excited vibrations in nonuniform flow is still in its infancy and, given the growing demand for oil exploration in deeper waters, a better quantitative understanding of the effect of shear in the flow on vortex-excited vibrations is essential.

A systematic experimental investigation has been initiated to understand the effect of flow and structural nonuniformities on vortex-excited vibrations at the University of Notre Dame's Hessert Center for Aerospace Research (Szewczyk *et al.* 1997). Uniform and tapered pivoted cylinders, cantilevers and tensioned cables are subjected to uniform and sheared

fluid loading in wind and water tunnels. The investigations focus on measuring response amplitudes and accelerations, lock-in ranges and power spectral density measurements of near-wake velocity fluctuations. While these experiments are expected to provide the much needed nonuniform flow data, they also provide a framework against which to evaluate the performance of a diffusive Van der Pol oscillator model (Balasubramanian & Skop 1997) in predicting vortex-excited vibrations in nonuniform flow scenarios. The vortex-excited dynamics of pivoted cylinders were studied first. Pivoted cylinders possess a single mode of response and hence are ideally suited to identify the important parameters in what is known to be a rather complex fluid–structure interaction mechanism. Here, we present salient features of the experimental investigation on the vortex-excited vibrations of uniform pivoted cylinders in uniform and shear flows. The experimental data are presented and compared with the results of the numerical predictions using the diffusive Van der Pol oscillator model. The preliminary results of the comparison between the numerical predictions and the experimental data were presented in Balasubramanian & Skop (1997). Here, details that were not presented in an earlier version of this paper are discussed in addition to new experimental evidence on the vortex-excited vibrations of uniform pivoted cylinders in linear shear flows and the corresponding numerical simulations.

2. EXPERIMENTAL INVESTIGATIONS

The experiments were conducted in a low turbulence in-draft wind tunnel that was 2·0 m long and had a square cross-section measuring 0·61 m $\times$ 0·61 m. The tunnel has an inlet contraction ratio of 20·6:1 with 12 antiturbulence screens. The flow was driven by an eight-bladed fan connected to an 18·6 kW AC induction motor. The speed capability of the tunnel ranged from 3 to 30 m/s and experiments were conducted at velocities ranging from 4 to 12 m/s. The turbulence intensity in this velocity range was less than 0·05%. A characteristic uniform velocity profile in the vertical direction recorded at the centerline of the wind tunnel is shown in Figure 1(a). The origin of the spanwise scale, denoted by z, corresponds to the top of the test-section, as seen in Figure 2.

A vertical shear flow was generated by employing an S-shaped screen upstream of the test-section. The shear screen (Elder 1959), originally used by Fiscina (1977) and later by Anderson (1994), was designed to provide a linear shear profile with turbulence intensities as low as 0·2%. Velocity profiles recorded at the centerline of the test-section are shown for two orientations of the shear screen in Figure 1(b, c). Also shown in Figure 1(d) is a quasilinear shear profile obtained from an identical but older shear screen.

The model cylinder used in the experiments was made from wood of density 540 kg/m^3. The cylinder had an outer diameter of 0·0572 m and a wall thickness of 0·0095 m, resulting in a mass per unit length of 0·77 kg/m. The cylinder was 0·601 m long and spanned the depth of the test-section. The model was pivoted on a bearing at the top of the test-section and the stiffness of the pivoted cylinder was increased by attaching two linear springs ($K = 1988$ N/m each) transversely to a sting protruding from the bottom of the cylinder as shown in Figure 2. The stiffness, and hence the natural frequency, of the pivoted cylinder was increased to enable vortex excitation within the limits of the achievable flow speeds in the wind tunnel. Constrained by the pivot at the top and by the springs at the bottom, the cylinder was capable of motion in the transverse direction only. The natural frequency of oscillation in the cross-flow direction and the system-damping ratio was recorded for the different experiments and are summarized in Table 1.

Measurements of the lateral displacement of the tip of the sting were made using an opto-electronic sensor. A horizontal laser light beam was directed at a small mirror mounted on the tip of the sting. The light beam was reflected at an angle of 45° from the

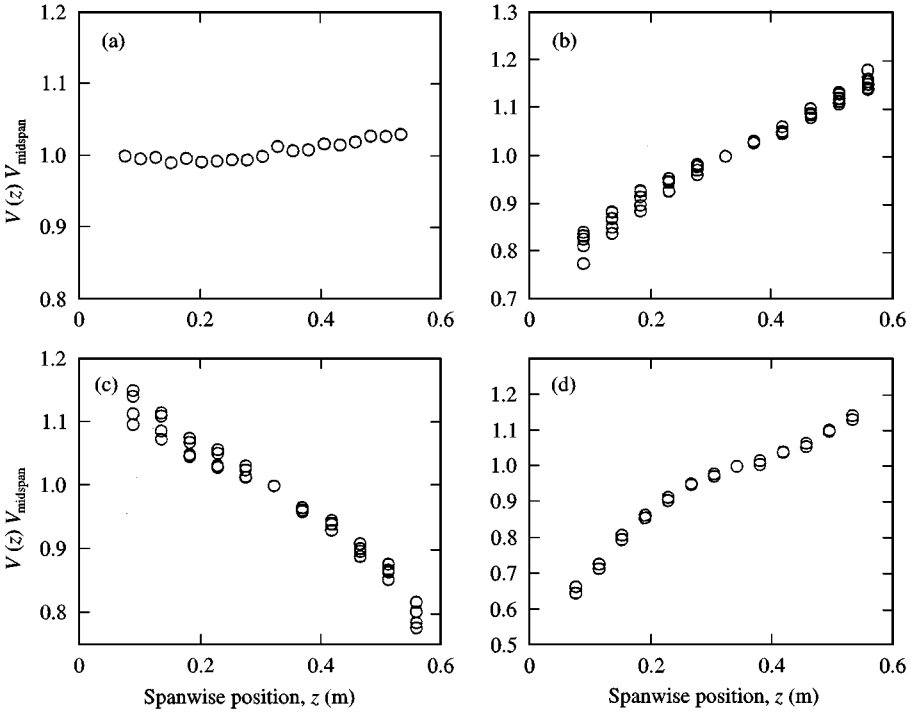

Figure 1. Experimentally recorded velocity profiles: (a) uniform flow; (b) linear shear profile with $V_{\max}$ at $z = L$; (c) linear shear profile with $V_{\max}$ at $z = 0$; (d) quasilinear shear flow.

mirror through a condensing lens onto a Graseby Optronics Model 1233 1·0 cm × 1·0 cm tetra-lateral detector. The signal from the lateral effect detector was then digitized and converted to tip displacements. The absence of displacements in the in-line mode was confirmed by analyzing the signal from the tetra-lateral detector. Measurements of flow velocity in the wind tunnel were made using a Pitot static tube connected to an electronic manometer. During the experiments the pitot tube was placed at a distance of 0·8 m forward of the cylinder and a distance of 0·53 m from the top of the tunnel. The position of the pitot tube was chosen so that it did not interfere with the flow pattern incident on the test cylinder. The wind tunnel blockage in these experiments was 9·3% and blockage correction was deemed unnecessary.

Hot-wire measurements of the near-wake velocity fluctuations due to vortex shedding were made using Dantec 55P01 single-wire probes. The probes had a tungsten wire sensor of 5 μm diameter and were operated in a constant-temperature mode with a TSI (IFA 100) anemometer. In an effort to sample the near wake at two spanwise locations at the same time, two probes vertically separated by 0·0254 m were used in tandem. The probes were mounted on a digitally controlled two-degree-of-freedom traverse mechanism. The hot-wire assembly was placed at a distance of two diameters downstream and 0·65 diameter away from the centerline of the cylinder. Power spectral densities and time histories of the near-wake velocity fluctuations were obtained at numerous spanwise positions along the cylinder. The power spectral densities were based on 30 ensembles of 1024 samples acquired at a sampling rate of 400 Hz for a total sample time of 76·8 s.

An issue of concern in these experiments was the effect of the opening on the floor of the test-section that was made for structural amplitude measurements (see Figure 2).

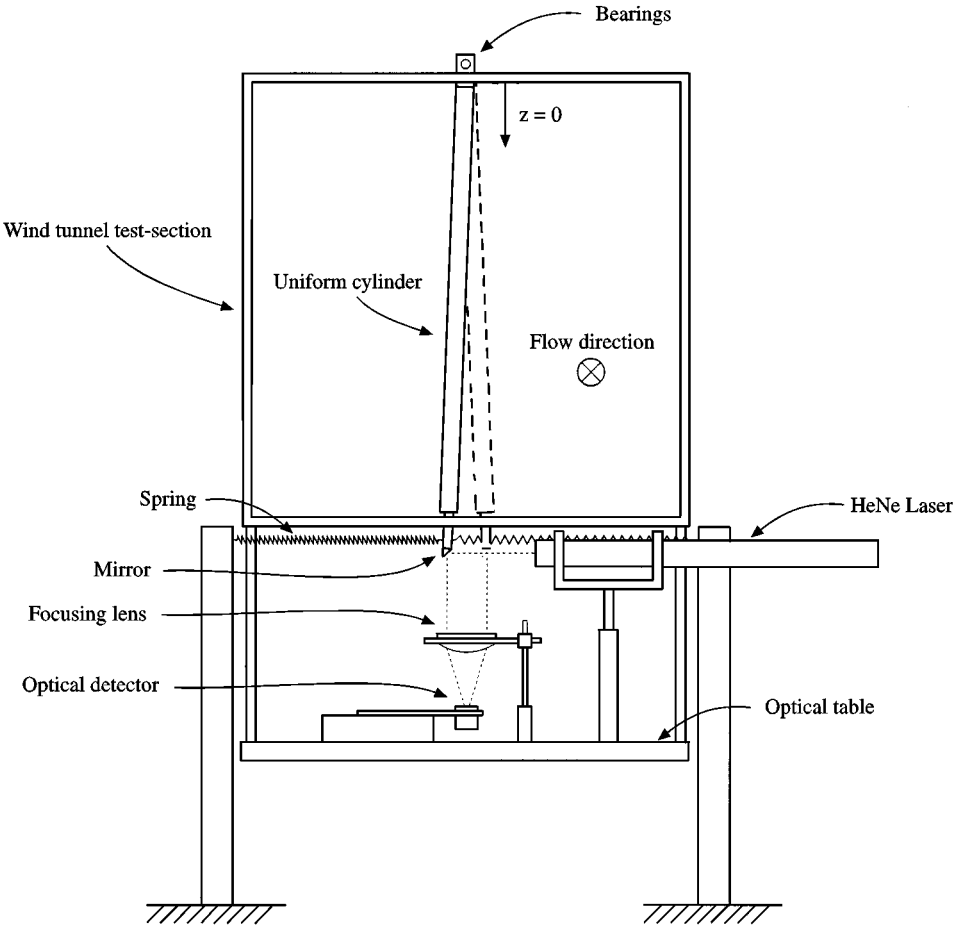

Figure 2. Cross-sectional schematic of the uniform pivoted cylinder in the wind tunnel.

TABLE 1

Experimentally measured natural frequencies and system damping ratios for the uniform pivoted cylinder

Velocity profile	Natural frequency (Hz)	System damping ξ
Uniform flow	20·2	0·0031
Linear shear flow V_{max} at $z = 0$	19·8	0·0031
Linear shear flow V_{max} at $z = L$	19·8	0·0031
Quasilinear shear flow V_{max} at $z = 0$	20·2	0·0031

The suction caused by this slot could seriously impact the flow quality in the test-section. The in-flow due to the slot was reduced by using a tape and foam seal during the experiments. Turbulence intensity measurements were made both upstream and downstream of the cylinder location for the uniform flow case, with the slot partially open (experimental conditions) and closed, to gauge the effect of this opening on the flow field.

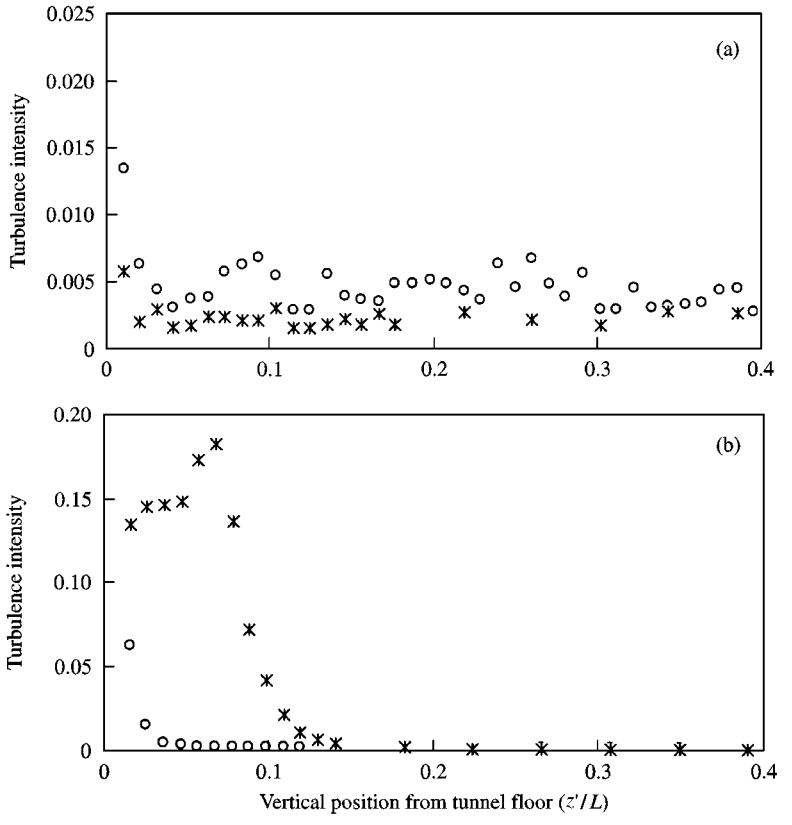

Figure 3. Turbulence intensities measured (a) upstream and (b) downstream of the cylinder location for uniform flow: ○, data recorded with the slot completely closed; ∗, s data recorded with the slot partially closed, as was the case in the experiments.

The measurement location was three diameters upstream of the cylinder centerline and two diameters downstream of the cylinder centerline. The turbulence intensity data, shown in Figure 3, indicate that the opening on the floor of the test-section had little impact if any on the flow quality upstream of the cylinder. Downstream of the slot, the turbulence intensity data indicate that the in-flow from the slot affects flow quality very close to the bottom of the test-section. The measured turbulence intensities for $0{\cdot}0 < z' < 0{\cdot}12$ ($z' = L - z$; L is the depth of the test-section) are about one order of magnitude higher when the slot is open. However, the rapid drop-off in turbulence intensities for $z' > 0{\cdot}12$ is indicative of the fact that the slot did not greatly affect the near-wake flow dynamics of the cylinder. A complete discussion of the vortex dynamics in the near wake of finite length cylinders in turbulent flows has been reported by Farivar (1981). Farivar reports increased turbulence intensities in a region close to the tip of the cylinder, but no significant increase in turbulence intensities away from the end of the cylinder. The turbulence intensity data from the current experiments appear to confirm this trend. Turbulence intensities recorded upstream of the cylinder location for the shear flow scenario are qualitatively similar to those recorded in the uniform flow experiment. Turbulence intensities were not recorded downstream of the cylinder location for the shear flow cases, but it is assumed that the qualitative similarity in the turbulence intensities measured upstream of the cylinder between the uniform and shear flow cases extends to the downstream turbulence intensities as well.

3. NUMERICAL MODELING

The numerical simulation of the vortex-excited dynamics of a uniform pivoted cylinder in uniform and shear flows was accomplished by numerically integrating the equation of motion for a pivoted cylinder under fluid loading due to vortex shedding. The governing equation of motion for a pivoted cylinder was developed in terms of its angular displacement θ as

$$\frac{\mathrm{d}^2\theta}{\mathrm{d}t^2} + 2\xi\omega_n\frac{\mathrm{d}\theta}{\mathrm{d}t} + \omega_n^2\theta = \frac{\rho D}{2I}\int_0^L V^2 C_L z \,\mathrm{d}z, \tag{1}$$

where t is the time and z the axial coordinate along the cylinder. The system damping ratio is represented by ξ, the flow velocity by V and $\omega_n\,(=2\pi f_n)$ is the system's natural frequency. The length of the cylinder subjected to fluid loading is defined as L, and D is the cylinder diameter. The total inertia of the system is denoted by I and includes the inertia of the transverse springs that were used to increase the stiffness of the system. The total inertia of the system and its natural frequency have been determined using a lumped mass formulation following Thomson's (1988) development of the effect of spring mass on the natural frequency of a spring–mass system. Using this lumped mass formulation, the natural frequency of the spring-stiffened pivoted cylinder is expressed as

$$\omega_n^2 = \frac{2KL_1^2 + \int_0^L mgz \,\mathrm{d}z}{\int_0^L mz^2 \,\mathrm{d}z + \frac{2}{3}m_S L_1^2}, \tag{2}$$

where K is the spring constant of the springs, $L_1 = 0{\cdot}656$ m is the distance from the pivot to the point of attachment of the springs, and g is the acceleration due to gravity. The mass per unit length of the cylinder is denoted by m, and m_S is the lumped mass of the spring and the sting to which it is attached. The natural frequency is computed to be 20·6 Hz and is in good agreement with the experimentally recorded natural frequencies listed in Table 1.

In equation (1), the fluid forcing on the pivoted cylinder is expressed as a moment of the lift force caused by vortex shedding. The fluctuating lift coefficient, $C_L(z, t)$, is expressed as

$$C_L(z, t) = Q(z, t) - \frac{2\alpha}{\omega_S(z)}\frac{z}{D}\frac{\mathrm{d}\theta}{\mathrm{d}t}, \tag{3}$$

where $\omega_S(z) = 2\pi f_S(z)$ is the vortex-shedding frequency. The lift force due to vortex shedding as expressed in equation (3) comprises both an excitation term $Q(z, t)$, that represents the periodic nature of the vortex-excited lift force and a stall term proportional to the time rate of change of the structural displacement, with α described as the stall parameter. The stall term has been introduced into the expression for the vortex-excited lift force to account for the asymptotic self-limiting structural response at zero structural damping by Skop & Balasubramanian (1997). The excitation component of the lift coefficient $Q(z, t)$ is taken to satisfy a diffusive Van der Pol equation given by

$$\frac{\partial^2 Q}{\partial t^2} - \omega_S G(C_{L0}^2 - 4Q^2)\frac{\partial Q}{\partial t} + \omega_S^2 Q - v_t\frac{\partial^3 Q}{\partial z^2 \partial t} = \omega_S F\frac{z}{D}\frac{\mathrm{d}\theta}{\mathrm{d}t}, \tag{4}$$

and has been shown to arise as a leading-order approximation to the vortex-shedding instability mechanism.

In equation (4), G and F are parameters that are to be evaluated from the mass and damping properties of the system being modeled. The r.m.s. value of the lift coefficient for a stationary uniform cylinder in uniform flow is given by C_{L0} and is taken to be constant and equal to 0·28, for this Reynolds number range, following Protos *et al.* (1968). The

coefficient of the diffusive term is given by ν_t and has been termed by Skop & Balasubramanian (1995) to be a turbulent kinematic viscosity. Skop & Balasubramanian (1995) and Balasubramanian & Skop (1996) have obtained a linear relationship between the turbulent kinematic viscosity and a parameter, β, that quantifies the shear in the flow. The shear parameter is expressed in dimensionless form as

$$\beta = \frac{D_{\text{ref}}}{\omega_{S,\max}} \left| \frac{\mathrm{d}\omega_S}{\mathrm{d}z} \right|, \tag{5}$$

where $\omega_{S,\max}$ is the maximum vortex-shedding frequency along the span of the cylinder and D_{ref} is the cylinder diameter D. The linear relationship between the shear parameter and the turbulent kinematic viscosity was obtained by matching the cellular vortex-shedding patterns from stationary uniform cylinders in linear shear flows and is given by

$$\nu_t = 0{\cdot}013 L^2 \omega_{S,\max} \beta. \tag{6}$$

The evaluation of the parameters G and F is all that remains to complete the model description. For this, the reduced mass parameter μ has to be evaluated; It is defined as the ratio of fluid to structural masses and is given by

$$\mu = \frac{\rho D^2}{8\pi^2 S^2 m}, \tag{7}$$

which, for our experiments, yields $\mu = 0{\cdot}001478$, based on a Strouhal number of $S = 0{\cdot}21$. Using the experimentally measured damping ratio from Table 1, the reduced damping, S_G, is evaluated as $S_G = \xi/\mu = 2{\cdot}09$. The computation of G and F follows the method employed by Skop & Balasubramanian (1997) and they are found to be $G = 0{\cdot}307$ and $F = 2{\cdot}67$ based on a stall parameter value of $\alpha = 0{\cdot}183$. Equations (1) and (4) are discretized and numerically integrated in time using a fourth-order Runge–Kutta technique for the excitation range of flow velocities. Steady-state values of the angular displacement are obtained and converted into tip displacements A ($= L\theta$) for comparison with the experimental data. Details of the discretization and numerical integration are presented in Balasubramanian & Skop (1997).

4. RESULTS AND ANALYSIS

The dynamics of a uniform pivoted cylinder undergoing vortex-excited vibrations are presented in terms of structural amplitudes of vibration as a function of the flow velocity and as power spectral density plots of the near-wake velocity fluctuations during lock-in. The results of the numerical simulations of the experiments using the coupled equations of motion are presented and compared with the experimental results. The results for a uniform cylinder in uniform flow are presented first, followed by the uniform cylinder in shear flow cases.

4.1. Uniform Cylinder in Uniform Flow

The study of the dynamics of a uniform pivoted cylinder undergoing vortex-excited vibrations in a uniform approach flow provides a reference frame to evaluate the current experimental investigation in relation to the available experimental evidence on vortex-excited vibrations in uniform flow scenarios.

In the experimental investigation, the flow velocity was increased incrementally and time histories of displacement, acceleration and near-wake velocity fluctuations were recorded at

each velocity. Power spectral density measurements of the near-wake velocity fluctuations were recorded at various spanwise positions at different velocities. Analysis of the time histories of the optically measured tip displacement of the bottom of the pivoted cylinder, $A = L\theta$, indicates that the vortex-shedding frequency locks-on to the cylinder natural frequency at a reduced velocity of $V_r = 4{\cdot}65$. Here, the reduced velocity is defined as $V_r = V/f_n\ D$ and f_n is the experimentally determined natural frequency of the pivoted uniform cylinder. The displacement time histories, shown in Figure 4, reveal that at the onset of lock-in the cylinder response displays significant amplitude modulation. This modulation disappears as the amplitude of vibration increases with reduced velocity and reappears when the cylinder exits lock-in at around $V_r = 5{\cdot}50{\cdot}$ Amplitude modulation has been observed and reported in other experimental investigations (Brika & Laneville 1993). The maximum response amplitude occurs at a reduced velocity of $V_r = 5{\cdot}30$ and corresponded to a detuning ratio of 1·13 between the inherent vortex-shedding frequency and the cylinder vibration frequency. The maximum peak-to-peak response amplitude is found to be $2A/D = 0{\cdot}36$. The modally scaled maximum response amplitude (Skop & Griffin 1975) is $2\ (A/D)_{\text{scaled}} = 0{\cdot}28$ and compares very well with other available experimental amplitude data and the least-squares best fit (Skop & Balasubramanian 1997). The experimentally measured detuning ratio of 1·13 from the current experiment is approximately 10% lower than the least-squares best fit value of 1·22 obtained from the least-squares best fit to the detuning data in Skop & Balasubramanian (1997).

In a uniform flow, the diffusive term in the Van der Pol oscillator drops out and results in the lift coefficient being a function of time alone. The coupled set of equations, equations (1) and (4), were numerically integrated for velocities ranging from 5·00 to 8·00 m/s. The experimentally observed response amplitudes and the numerically simulated response amplitudes are shown in Figure 5. The experimental and model results are in good agreement in terms of the maximum amplitude of displacement. However the reduced velocity at which this maximum occurs is higher in the model predictions. This offset is the result of the difference in the frequency ratio used in the model and that observed in the experiments. The numerically predicted response amplitude curve corrected for the 10% difference in the frequency ratio (a corresponding 10% shift in the reduced velocity scale) is also shown in Figure 5. The corrected curve is in very good agreement with the experimental data. The numerical model predicts a slightly wider lock-in range compared to that observed in the experiments.

As part of the experimental investigations, power spectral density (PSD) measurements of the near-wake velocity fluctuations were recorded at various spanwise positions at different reduced velocities. The effect of cylinder vibration on the near-wake velocity fluctuations is observable from these power spectral density measurements. At a reduced velocity of $V_r = 4{\cdot}65$, the amplitude of cylinder vibration is very small and the cylinder is on the verge of experiencing lock-in. The experimentally recorded PSDs, as seen in Figure 6, display peaks at the natural frequency of the cylinder over a large extent of the span. At a reduced velocity of $V_r = 4{\cdot}65$, the inherent vortex-shedding frequency is computed to be $f_s = 19{\cdot}8$ Hz, based on a Strouhal number of $S = 0{\cdot}21$. PSD peaks at this inherent vortex-shedding frequency are seen at the pivoted end of the cylinder. The extreme sensitivity of the near wake to small-amplitude vibrations of the cylinder is evident. Also shown in Figure 6 is the experimentally recorded PSDs at a reduced velocity of $V_r = 5{\cdot}10$ as a function of the spanwise location along the cylinder. The pivoted cylinder is under lock-in at this reduced velocity. The near-wake responds at the cylinder's natural frequency and the peaks are sharper than at a reduced velocity of $V_r = 4{\cdot}65$. The inherent vortex-shedding frequency of $f_s = 21{\cdot}4$ Hz is observable at the pivoted end. At a reduced velocity of $V_r = 5{\cdot}30$, the cylinder is responding close to its maximum amplitude. The PSDs of the near wake at this reduced

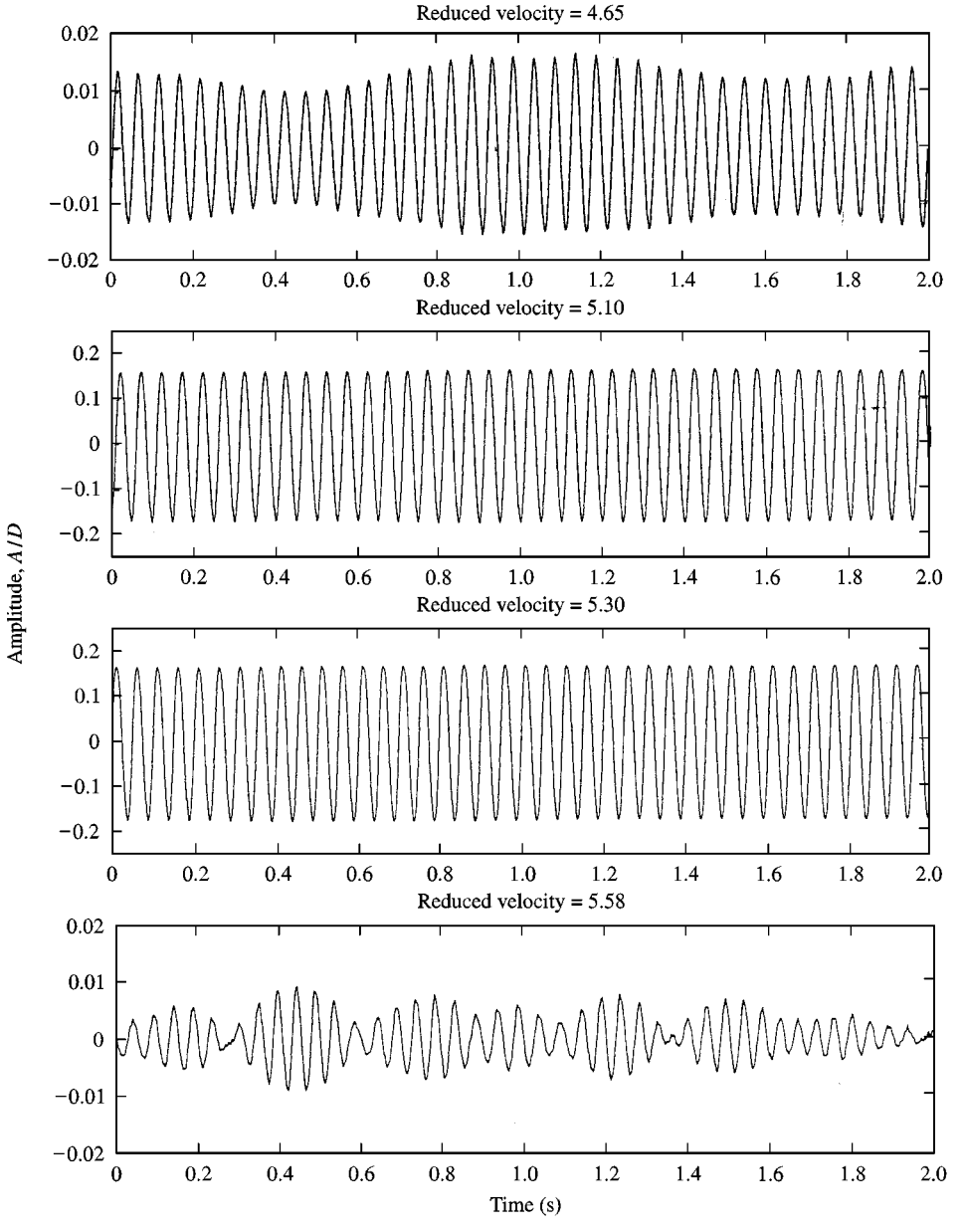

Figure 4. Displacement time histories of the tip displacement of a uniform cylinder in uniform flow at different reduced velocities.

velocity, as seen in Figure 7, indicate that vortices are being shed at the cylinder natural frequency and the peaks of the velocity fluctuations are very sharp and are indicative of the amplification in the fluctuating lift forces due to increased energy transfer from cylinder vibration to the near wake.

Ramberg & Griffin (1976) have reported the existence a modal scaling of the near wake due to vortex-excited vibrations. Skop & Balasubramanian (1997) have used the experimental findings of Ramberg & Griffin (1976) in the development of the fluctuating lift

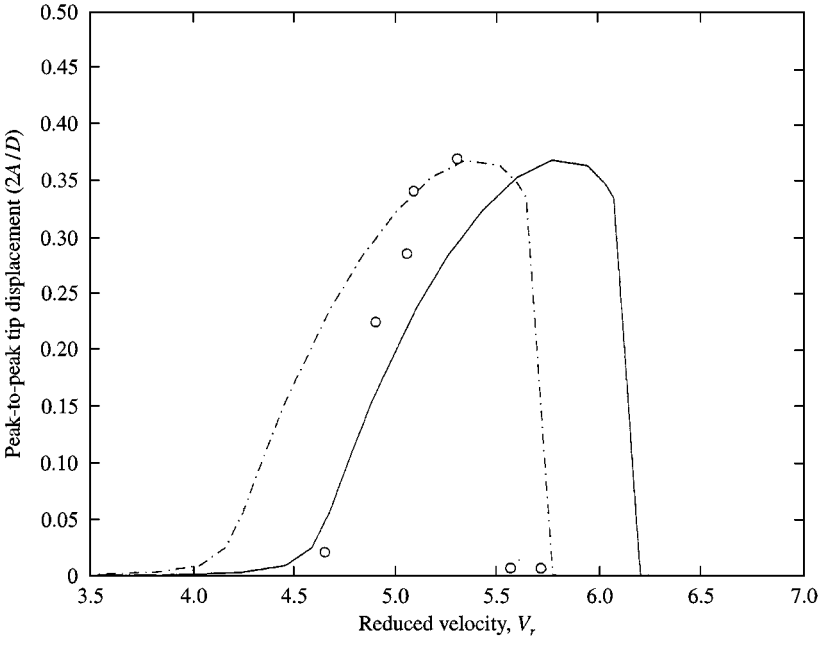

Figure 5. Response amplitude of a uniform pivoted cylinder undergoing vortex-excited vibrations in an uniform flow: ○, experimentally recorded response amplitudes —, the numerically predicted response amplitude curve; –·–·–, the predicted curve corrected for the difference in the frequency ratio between experiment and model.

coefficient as a modal expansion in their model. A close inspection of the PSD data from the current experiment indicates that the amplitudes of the peaks appear to increase with increasing distance from the pivot, indicating a modal scaling of the wake. However, it must be noted that to ascertain this modal scaling effect accurately, PSDs must be recorded at the location in the near-wake velocity fluctuations have maximum amplitude. The current experiments were not designed to accomplish that. Further, the effect of the in-flow from the slot on the near-wake velocity fluctuations is of unknown magnitude.

In the numerical simulations, the PSDs of the excitation component of the fluctuating lift coefficient $Q(z, t)$ were computed using a Fast Fourier transform. PSDs were computed at 50 spanwise locations and are shown in Figure 7 for the case when the cylinder is responding at its maximum amplitude. The numerically predicted PSDs are in excellent agreement with the experimentally recorded PSDs under lock-in. The numerical model accurately predicts the transition of the near wake from the cylinder natural frequency to the inherent vortex-shedding frequency close to the pivot.

4.2. Uniform Cylinder in a Linear Shear Flow

A uniform cylinder in a linear shear flow provides for a linear variation in the vortex-shedding frequency along the span of the cylinder. A very important feature of this variation from the point of view of vortex-excited vibrations is that some part of the cylinder could be under lock-in conditions over a larger velocity range than in a uniform flow. Two variations of the linear shear flow over a uniform cylinder were studied. The shear flow was oriented such that the maximum velocity occurred at the free end of the pivoted cylinder in one of the experiments, whereas in the other experiment, the shear screen was oriented such that the maximum velocity occurred at the pivoted end of the cylinder.

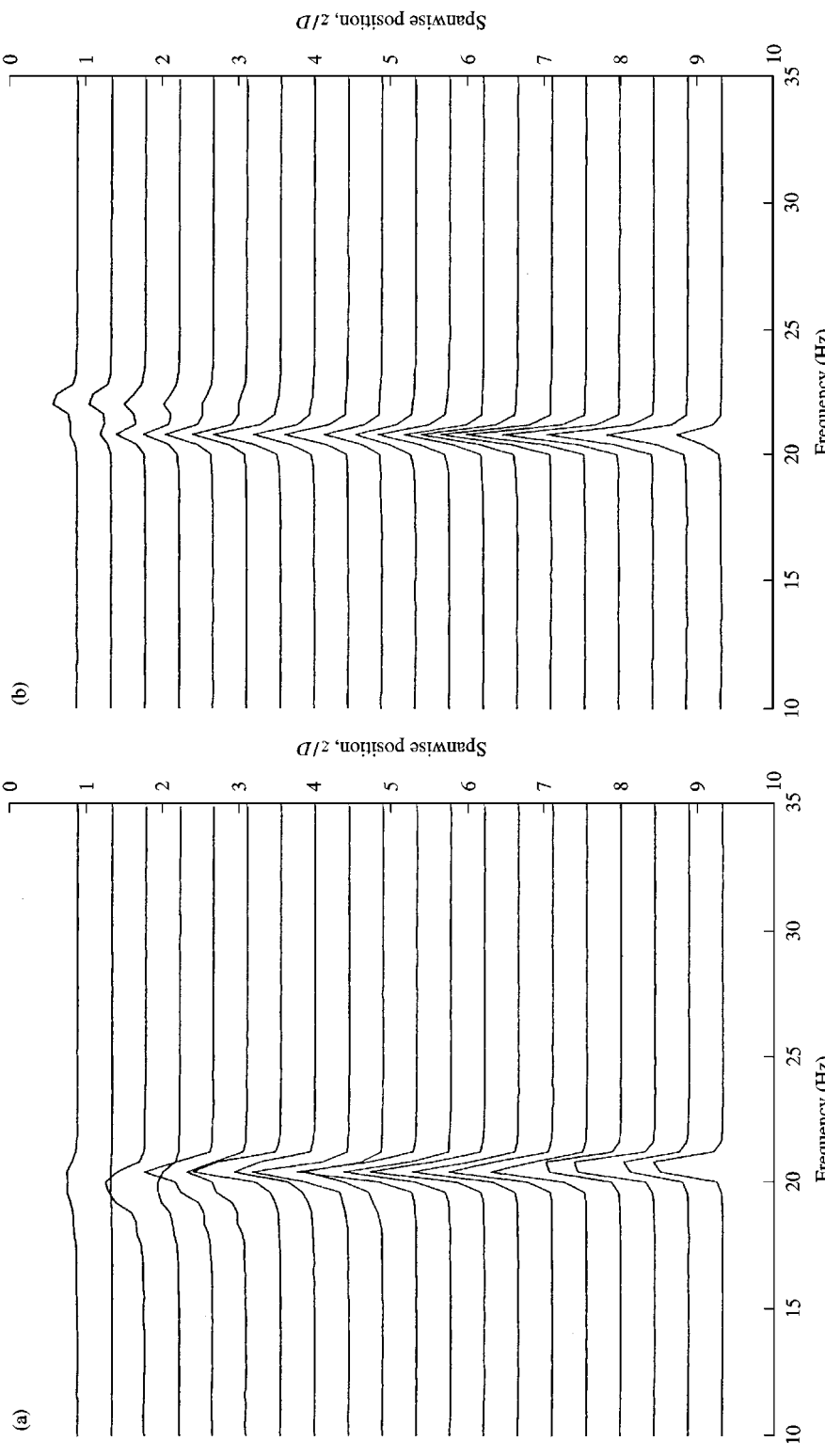

Figure 6. Experimentally recorded power spectral densities of the velocity fluctuations in the near wake of a uniform pivoted cylinder in an uniform approach flow at reduced velocities of (a) $V_r = 4{\cdot}65$ and (b) $V_r = 5{\cdot}10$.

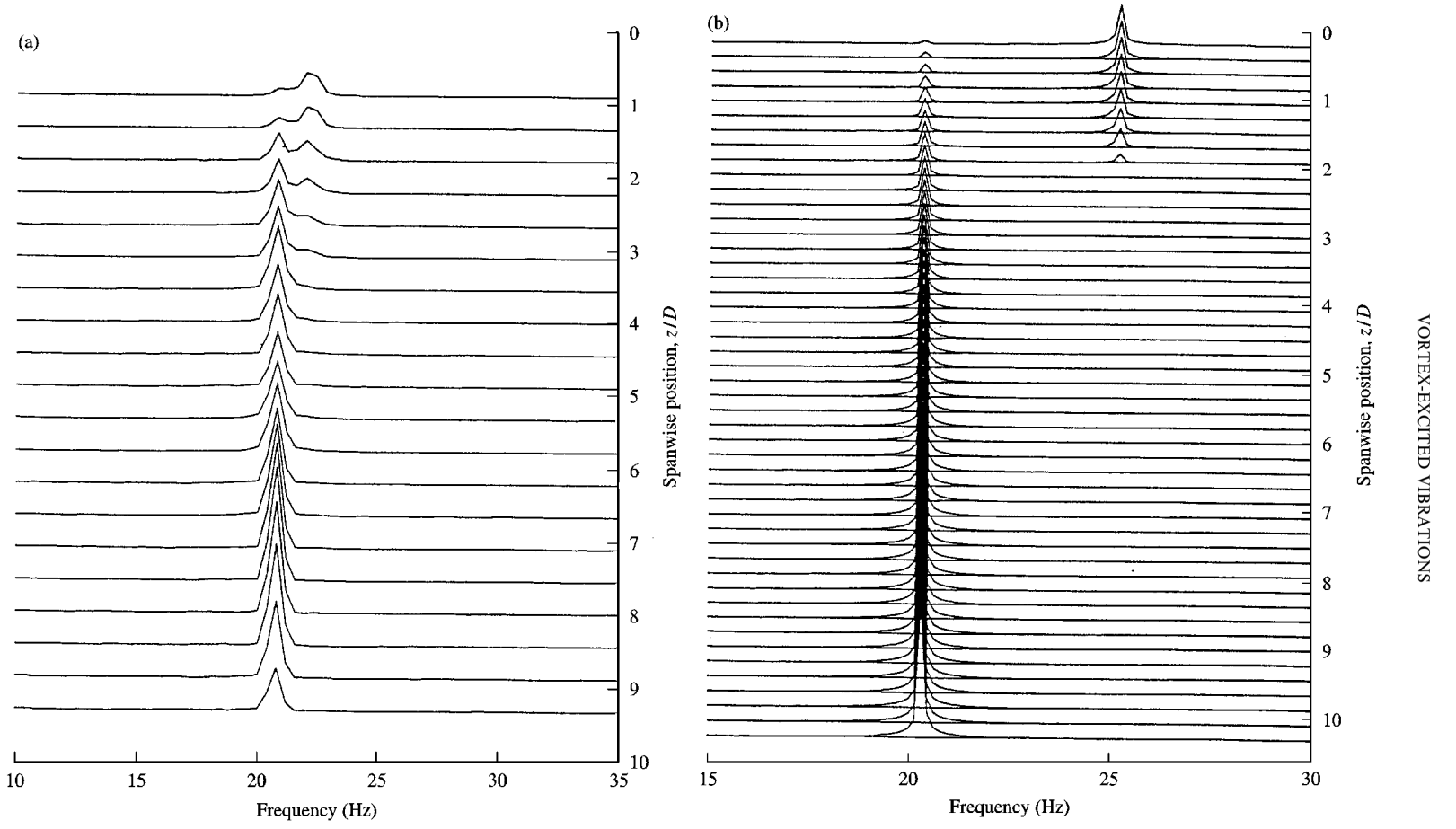

Figure 7. Experimentally recorded PSDs (a) of the velocity fluctuations in the near wake of a uniform cylinder at $V_r = 5{\cdot}30$ and (b) the numerically predicted PSDs of the excitation component of the lift coefficient at $V_r = 5{\cdot}90$. The reduced velocities correspond to the cylinder responding at maximum amplitude to vortex-excited vibration in uniform flow.

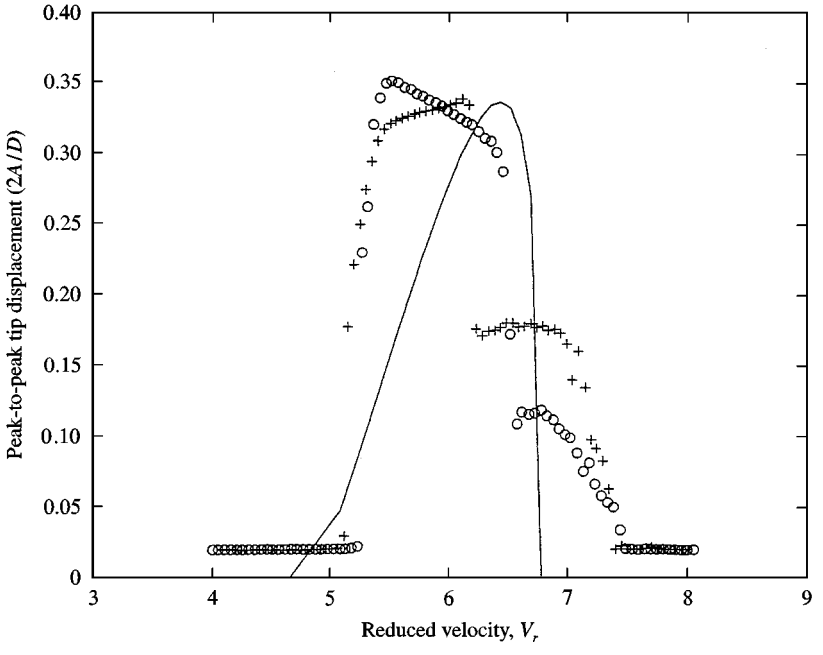

Figure 8. Experimentally observed response amplitudes of a uniform pivoted cylinder undergoing vortex-excited vibrations in a linear shear flow: ○, data recorded with increasing velocity; +, data recorded with decreasing velocity. The solid line is the numerically predicted response amplitude curve.

4.2.1. *Maximum flow velocity at the free end*

With the shear screen oriented such that the maximum velocity occurs at the bottom of the test-section, the experimentally recorded amplitudes of vibration with increasing and decreasing velocities are shown in Figure 8. For this case, the shear parameter is constant and given by $\beta = 0{\cdot}033$. The cylinder is observed to go into lock-in at a reduced velocity of $V_r = 5{\cdot}30$. The reduced velocity is defined in terms of the velocity recorded at the pitot position of $z = 0{\cdot}53$ m. The cylinder amplitude increases rapidly for small increases in the reduced velocity and reaches a maximum value of $2A/D = 0{\cdot}35$ at a reduced velocity of $V_r = 5{\cdot}50$. The amplitudes then decrease slowly with increasing reduced velocity until a reduced velocity of $V_r = 6{\cdot}50$ is reached. At this value of the reduced velocity, there is an abrupt drop in amplitude to a value of $2A/D = 0{\cdot}13$. With further increases in reduced velocity, the cylinder amplitude decreases slowly until the cylinder goes out of lock-in at a reduced velocity of $V_r = 7{\cdot}50$.

When the reduced velocity was decreased from a value of $V_r = 8{\cdot}10$, the cylinder displays lock-in behavior at a reduced velocity of $V_r = 7{\cdot}50$ and the amplitude of vibration increases to a value of $2A/D = 0{\cdot}20$ as the reduced velocity reaches a value of $V_r = 7{\cdot}10$. From a reduced velocity of 7·10 to a reduced velocity of 6·20, the displacement amplitude remains a constant. At a reduced velocity of 6·20, the response amplitude increases abruptly to a value of $2A/D = 0{\cdot}35$. Further decreases in reduced velocity result in lower response amplitudes till the cylinder finally exits lock-in at a reduced velocity of $V_r = 5{\cdot}20$.

The numerical modeling of the current experimental set-up was performed using the linear best fit to the experimentally measured velocity data. The velocity profile was given by

$$V(z) = V_0(1{\cdot}0 + 0{\cdot}88z), \tag{8}$$

where V_0 is the velocity at $z = 0$. The natural frequency of the system was evaluated to be $f_n = 20{\cdot}6$ Hz and compares well with the experimentally measured natural frequency of 19·8 Hz. The numerically predicted response curve is shown in Figure 8 as a solid line. The numerical model predicts a maximum response amplitude of $2A/D = 0{\cdot}35$ at a reduced velocity of $V_r = 6{\cdot}50$· The predicted maximum response amplitude compares very well with the experimentally measured response amplitude. The reduced velocity at which the maximum amplitude occurs in the numerical simulations is higher compared to the experimental results. The experimentally recorded maximum amplitudes occur at different reduced velocities depending on whether the velocity was increased or decreased through the lock-in range. The model predicts a lock-in range of $\Delta V_r = 1{\cdot}70$ and is smaller than the experimentally recorded lock-in range.

Differences exist in the nature of the amplitude response of the cylinder with increasing and decreasing velocities. The primary difference is the reduced velocity at which the maximum amplitude occurs. The reasons for this difference are not readily apparent. This difference, however, adds credence to the large scatter that is observed in the compiled data from other experiments on the frequency ratio at which the maximum response amplitude occurs. Also, the low-amplitude secondary stable response at reduced velocities of $V_r \geq 6{\cdot}00$ is noteworthy. The amplitudes measured with increasing and decreasing velocities (for $V_r \geq 6{\cdot}00$) differ considerably and could be construed as evidence of response hysteresis. If this low amplitude, stable response were to be disregarded, then there is good agreement between the numerically predicted and experimentally observed lock-in ranges. One can speculate that the secondary response amplitude observed in the experiments is a higher order feature of vortex-excited vibrations in nonuniform flow.

4.2.2. *Maximum velocity at the pivoted end*

Reversing the orientation of the shear screen results in the pivoted cylinder being forced by a linear shear flow with the maximum flow velocity occurring at the pivoted end. For this case, the shear parameter was evaluated to be $\beta = 0{\cdot}031$. The experimentally recorded tip-displacement amplitudes of the uniform cylinder as a function of the reduced velocity are shown in Figure 9. The nature of the experimentally recorded response curves for both increasing and decreasing velocities are similar. In both cases, locked-in cylinder response is between the reduced velocities of 5·30 and 6·70. The maximum recorded response amplitude is $2A/D = 0{\cdot}25$ and occurs at a reduced velocity of $V_r = 5{\cdot}90$ for the increasing velocity case and at a reduced velocity of $V_r = 6{\cdot}10$ for the decreasing velocity case. The numerical simulation of the current experimental setup was accomplished using a linear best fit to the velocity profile given by

$$V(z) = V_0(1{\cdot}0 - 0{\cdot}54z). \tag{9}$$

The numerically predicted response amplitudes and the experimentally recorded response amplitudes are in close agreement. The numerically predicted maximum response amplitude of $2A/D = 0{\cdot}25$ occurs at a reduced velocity of 5·80 as seen in Figure 9. The range of lock-in predicted by the model compares very well with the experimentally recorded range of lock-in. The forcing moment and hence the response amplitudes of the pivoted cylinder with the maximum velocity occurring at the pivoted end are intuitively expected to be lower than with the maximum velocity at the free end. The amplitudes recorded in the experiments and by those predicted by the model are in line with this intuitive argument.

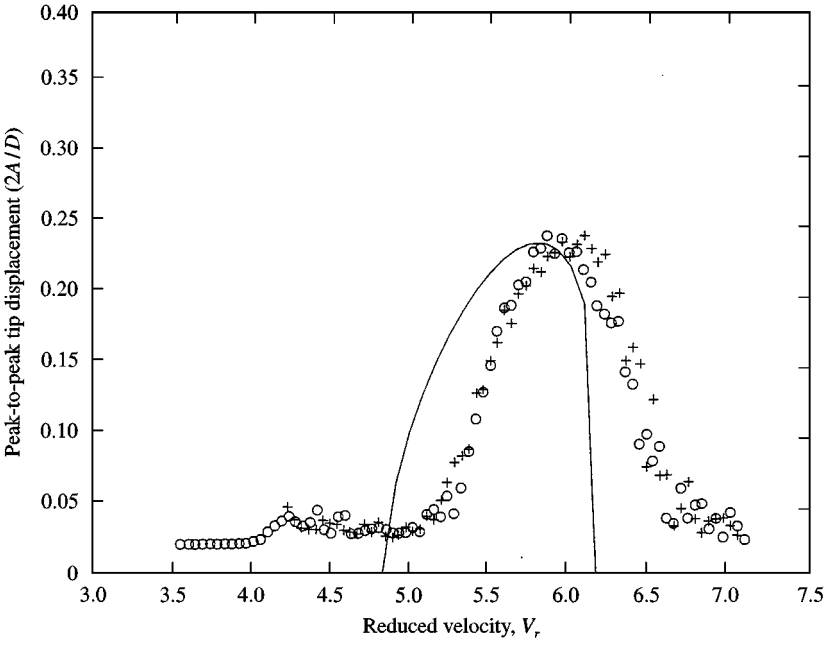

Figure 9. Experimentally recorded response amplitudes of a uniform pivoted cylinder undergoing vortex-excited vibrations in a linear shear flow: ○, data recorded with increasing velocity; +, data recorded with decreasing velocity. The solid line is the numerically predicted response amplitude curve.

4.3. Uniform Cylinder in a Quasilinear Shear Flow

The experimentally measured response amplitude of the uniform cylinder due to vortex excitation in a quasilinear shear profile (see Figure 1) is shown in Figure 10· In this experiment, the maximum flow velocity occurs at the free end of the pivoted cylinder ($z = L$). The lock-in range starts at a reduced velocity of $V_r = 5{\cdot}30$ and the maximum response amplitude of $2A/D = 0{\cdot}35$ also occurs at this reduced velocity. The response amplitudes decrease with increasing reduced velocity and the cylinder finally exits lock-in at a reduced velocity of $V_r \approx 6{\cdot}20$· The amplitudes recorded with decreasing velocity are consistent with the data recorded with increasing velocity.

The quasilinear shear profile was approximated by both a linear best fit and a bilinear best fit to the measured velocity data. The linear best fit was given by

$$V(z) = V_0(1{\cdot}0 + 1{\cdot}32z), \tag{10}$$

and the bilinear best fit by

$$\begin{aligned} V(z) &= V_0(1{\cdot}00 + 3{\cdot}81z), \quad z \leq 0{\cdot}19, \\ V(z) &= V_0(1{\cdot}44 + 1{\cdot}48z), \quad z \geq 0{\cdot}19. \end{aligned} \tag{11}$$

In the experimental determination of the velocity profiles, velocity data was recorded only over $0{\cdot}0762 \leq z \leq 0{\cdot}5375$ of the test-section. The best fits to the velocity data have been made applicable over the entire depth of the test-section ($0 \leq z \leq 0{\cdot}601$) and may prove to be significant approximations in this case.

The numerical simulation of the response of the uniform cylinder in a quasilinear shear flow to vortex-excited vibrations was performed with both the linear best fit to the velocity profile and the bi-linear best fit to the velocity data. The numerically predicted response

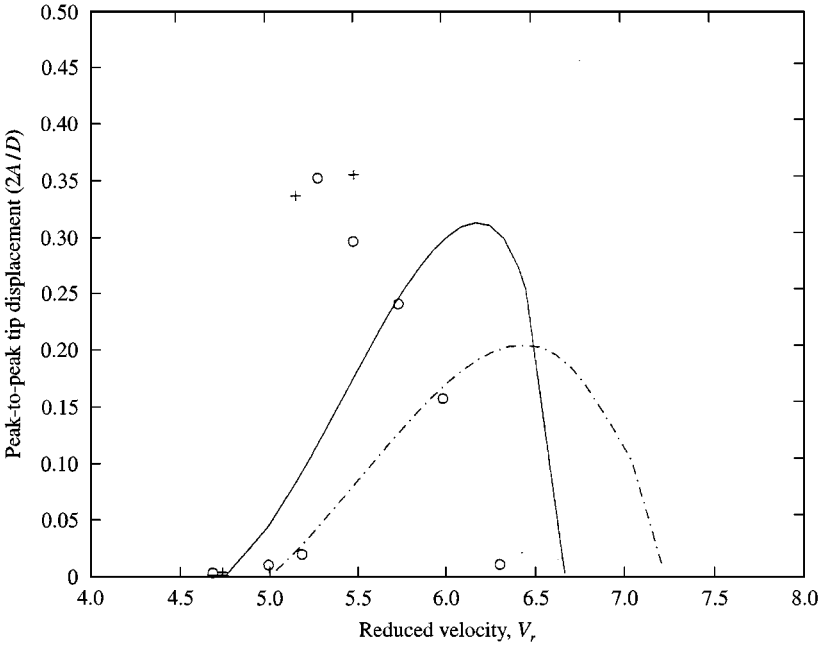

Figure 10. Peak-to-peak structural displacement of the uniform pivoted cylinder in a quasilinear shear flow: ○, +, experimentally recorded tip displacements with increasing and decreasing velocities, respectively; – · – · –, the numerically predicted response curve with the velocity profile represented by equation (10); —, the predicted response with equation (11).

amplitude curve using the linear best fit is shown in Figure 10 as a dashed line. The predicted lock-in range of $5{\cdot}00 \leq V_r \leq 7{\cdot}30$ is substantially larger than the experimentally recorded lock-in range. The maximum response amplitude predicted by the model is $2A/D = 0{\cdot}20$ and occurs at a reduced velocity of $V_r = 6{\cdot}50$. The agreement between the numerically predicted response amplitude curve and the experimental response amplitude is poor. The numerical simulations performed with a bilinear best fit predict a lock-in range of $4{\cdot}50 \leq V_r \leq 6{\cdot}70$ and a maximum response amplitude of $2A/D = 0{\cdot}31$ at a reduced velocity of $V_r = 6{\cdot}20$. The agreement between the numerical simulations and the experimental data is better than that with a linear best fit, and the numerically predicted lock-in range is substantially larger than the experimentally recorded lock-in range.

The bilinear velocity profile is a better representation of the experimentally recorded velocity profile and hence does a better job of replicating the fluid loading on the pivoted cylinder in the numerical simulations than does a linear best fit. The extreme sensitivity of the lock-in range and the response amplitude in the numerical simulations on the velocity profile used is not surprising. It can be expected that a more accurate representation of the measured velocity profile would result in even better agreement between the numerical predictions and the experimental data.

The experimentally recorded power spectral densities of the velocity fluctuations in the near wake of the uniform cylinder in a quasilinear shear flow are shown in Figure 11 for prelock-in and lock-in conditions. At a reduced velocity of $V_r = 4{\cdot}68$, the near wake is seen to respond at its inherent vortex shedding frequency. The near-wake response is broadband and cellular in nature. At a reduced velocity of $V_r = 5{\cdot}30$, the cylinder is under lock-in and the near wake responds at the cylinder natural frequency of 20·2 Hz. The broadband nature of the PSD peaks is replaced by sharp narrow-band responses. The numerically predicted

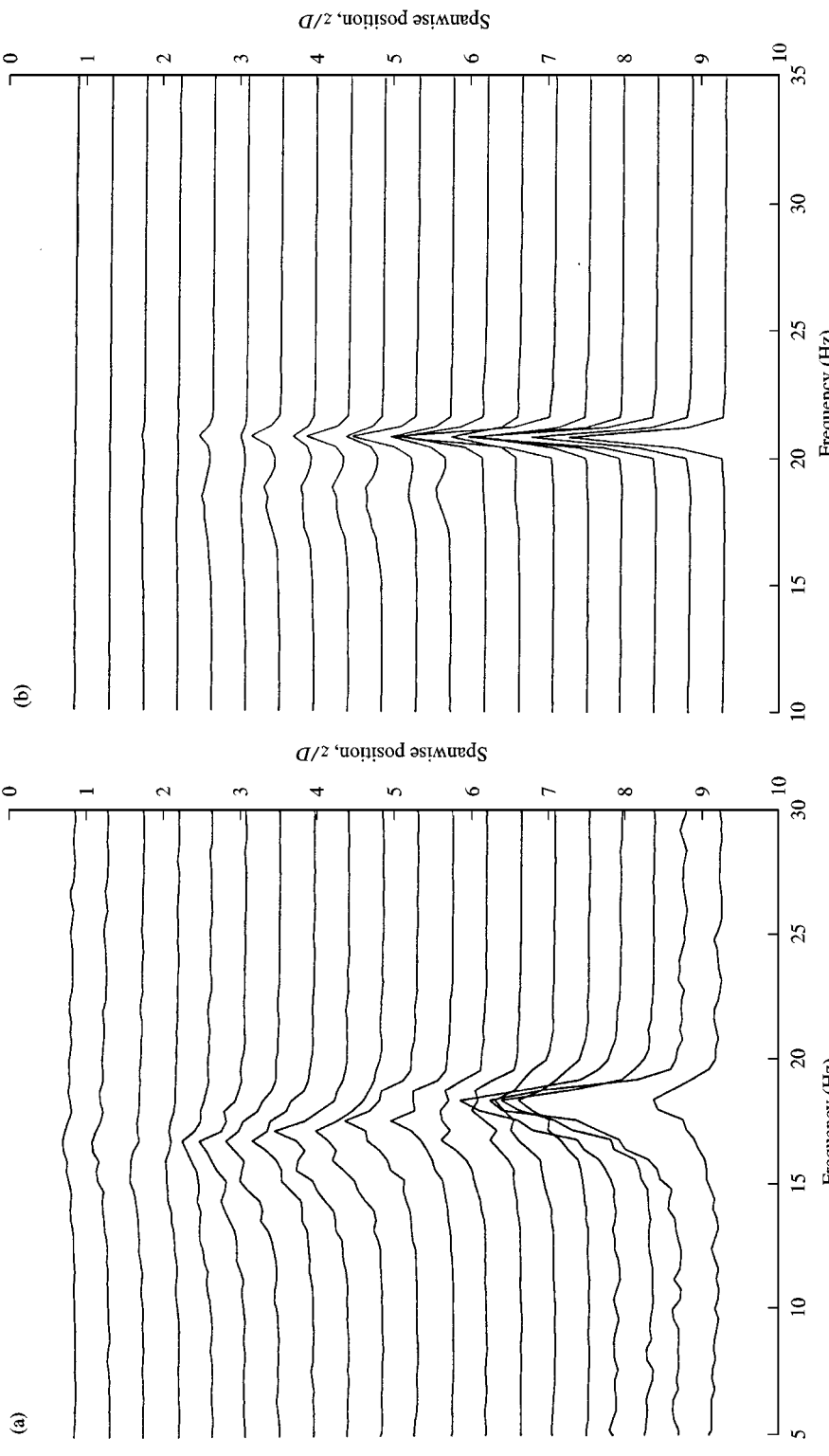

Figure 11. Experimentally recorded power spectral densities of the velocity fluctuations in the near wake of a uniform pivoted cylinder in a shear flow under (a) prelock-in and (b) lock-in conditions.

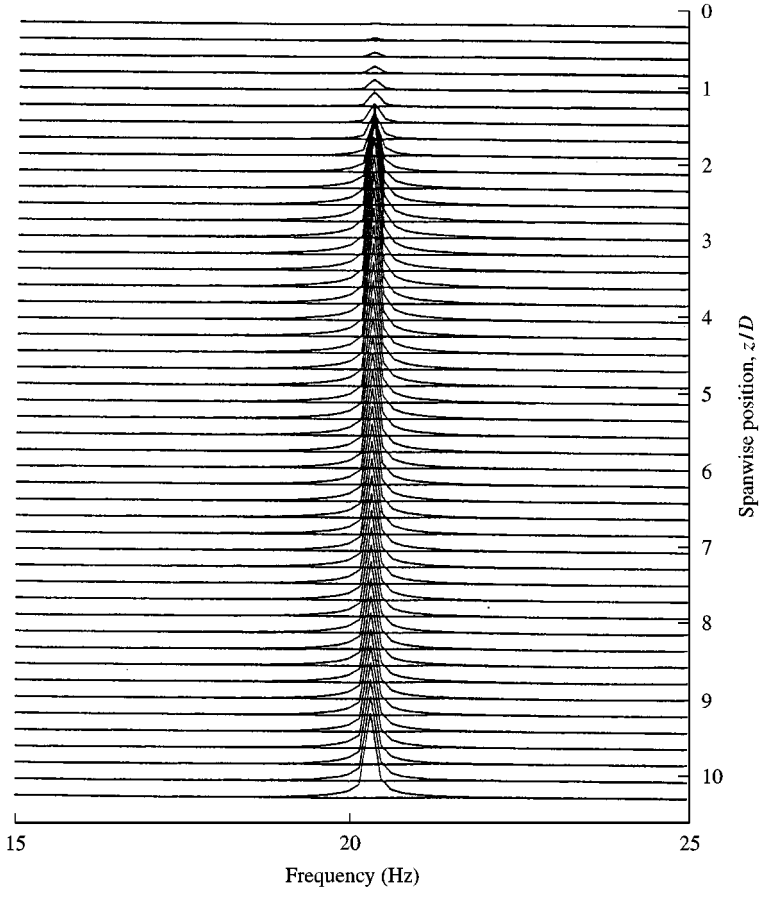

Figure 12. Waterfall plot of the power spectral densities of the excitation component of the fluctuating lift coefficient for a uniform pivoted cylinder undergoing vortex-excited vibrations in a shear flow.

power spectral densities of the excitation component of the lift coefficient are shown in Figure 12 for the uniform cylinder responding at its maximum response amplitude. The numerically predicted PSDs display good quantitative agreement with the experimental data.

5. CONCLUSIONS

The experimental investigations of the vortex-excited vibrations of uniform pivoted cylinders in uniform and shear flows indicate that the response amplitudes are primarily dependent on the structural properties of the cylinder. The experimentally recorded lock-in ranges for the uniform cylinder in the shear flow experiments are consistently higher than in uniform flow experiments, indicating that the lock-in range of reduced velocities is governed by the shear in the flow. The experimental amplitude data for one of the shear flow experiments (linear shear flow with maximum velocity at the free end) indicates the existence of a secondary stable response and hysteretic response behavior. Experiments to investigate the secondary stable response behavior are essential to characterize the phenomenon accurately.

The equation of motion of the pivoted cylinder forced, in part, by a diffusive Van der Pol equation representing the excitation component of the lift coefficient due to vortex shedding has been introduced as a successful model for vortex-excited vibrations in nonuniform flow fields. The results of the numerical simulations are in good agreement with the experimentally observed results for shear flows over uniform cylinders. The model has been shown to be successful in matching the maximum response amplitudes and the lock-in ranges. Principal observations made from the performance of the model can be summarized as follows.

The numerically predicted maximum response amplitudes occur at a higher reduced velocity than that experimentally observed, except for one of the experiments. The reason for this difference between the numerical model and the experiments can be attributed to the average value of the frequency ratio that is used in the model. The frequency ratio used in the model is obtained from data compiled from different experiments and, as seen in figure 4 in Skop & Balasubramanian (1997), show significant scatter. The current experimental data appear to confirm the trend. The frequency ratio at which the maximum amplitude occurs appears to be very sensitive to flow conditions as evidenced in the current experiments.

The numerically predicted response amplitude curves exhibit a sharp drop-off after the maximum amplitude is reached. The experimental data indicate slower fall-off after the maximum amplitude is reached. Reasons for this difference in the shape of the curves could have their origins in the leading-order nature of the model. The difference in the shape of the response curve could be due to the fact that while a diffusive Van der Pol oscillator is capable of matching the lock-in ranges and amplitudes, it comes up short of replicating the actual fluid-elastic instability mechanism. The numerical model is very sensitive to the shear gradient in the flow. The differences in the predicted response amplitudes with the linear and bilinear best fits to the quasilinear velocity data support this observation. The structural equation of motion is driven by the moment of the lift force and the amplitude of this driving moment governs the structural response. The amplitude of this moment is largely controlled by the value of the lift force at the free end of the cylinder. A linear best fit to the velocity data does not accurately model the fluid loading over the free end of the cylinder, resulting in poor agreement between the experimental and numerical results. Overall for its elementary nature, the model provides excellent agreement with the principal features of what essentially is a complex fluid–structure interaction problem.

ACKNOWLEDGEMENTS

The authors sincerely acknowledge the support of the U.S. Office of Naval Research under Grants nos. 0014-93-1-0438 and 0014-96-0756 for the work reported in this paper.

References

Alberéde, P. & Monkewitz, P. A. 1992 A model for the formation of oblique shedding and "Chevron" patterns in cylinder wakes. *Physics of Fluids* A **4,** 744–756.

Anderson, E. A. 1994 Effects of taper and splitter plates on the near wake characteristics of a circular cylinder in uniform and shear flow. Ph. D. Dissertation, University of Notre Dame, South Bend, IN, U.S.A.

Balasubramanian, S., Haan, F. L., Szewczyk, A. A. & Skop, R. A. 1998 On the existence of a critical shear parameter for cellular vortex shedding from cylinders in nonuniform flow. *Journal of Fluids and Structures* **12,** 3–15.

Balasubramanian, S. & Skop, R. A. 1996 A nonlinear oscillator model for vortex shedding from cylinders and cones in uniform and shear flows. *Journal of Fluids and Structures*, **10,** 197–214.

Balasubramanian, S. & Skop, R.A. 1997 Modeling vortex-excited vibrations of uniform cylinders in uniform and shear flow. *Proceedings of the fourth International Symposium on Fluid–Structure Interactions, Aeroelasticity, Flow-Induced Vibration and Noise* (eds M. P. Païdoussis *et al.*), AD-Vol. 53–1, pp. 121–126.

Brika, D. & Laneville, A. 1993 Vortex-induced vibration of a long flexible circular cylinder. *Journal of Fluid Mechanics* **250,** 451–508.

Chung, T. Y. 1987 Vortex-induced vibrations of flexible cylinders in sheared flows. Ph.D. Dissertation, Massachusetts Institute of Technology, Cambridge, MA, U.S.A.

Elder, J. W. 1959 Steady flow through nonuniform gauzes. *Journal of Fluid Mechanics* **5,** 355–368.

Farivar, Dj. 1981 Turbulent uniform flow around cylinders of finite length. *AIAA Journal* **19,** 275–281.

Fischer, F. J., Jones, W. T. & King, R. 1980 Current induced oscillations of Cognac piles during installation. In *Practical Experiences with Flow-Induced Vibrations* (eds E. Naudascher & D. Rockwell), pp. 570–581. Berlin: Springer-Verlag.

Fiscina, C. 1977 An investigation into the effects of shear on the flow past bluff bodies. M.S. Thesis, University of Notre Dame, South Bend, IN, U.S.A.

Goyder, H. G. D. 1997 Vortex-induced vibrations of chemical plant towers. *Proceedings of the fourth International Symposium on Fluid–Structure Interactions, Aeroelasticity, Flow-Induced Vibration and Noise* (eds M. P. Païdoussis *et al.*), AD-Vol. 53–1, pp. 113–120·

Griffin, O. M. 1982 Vortex shedding from cables and structures in a shear flow: state of the art. Naval Civil Engineering Laboratory Report CR 84.004.

Kim, Y. H., Vandiver, J. K. & Holler, R. A. 1985 Vortex-induced vibration and drag coefficients of long cables subjected to sheared flows. *Proceedings of the Fourth International Offshore Mechanics and Arctic Engineering Symposium*, Vol. 1, pp. 584–592. New York: ASME.

Protos, A., Goldschmidt, V. & Toebes, G. 1968 Hydroelastic forces on bluff cylinders. *ASME Journal of Basic Engineering* **90,** 378–386.

Ramberg, S. E. & Griffin, O. M. 1976 Velocity correlation and vortex spacing in the wake of a vibrating cable. *ASME Journal of Fluids Engineering* **98,** 10–18.

Sarpkaya, T. 1978 Fluid forces on oscillating cylinders. *ASCE Journal of Port, Waterway, Coastal and Ocean Engineering* **104,** 275–290·

Skop, R. A. & Balasubramanian, S. 1995 A nonlinear oscillator model for vortex shedding from a forced cylinder in a shear flow. Part 2: shear flow and axial diffusion. *International Journal of Offshore and Polar Engineering* **5,** 256–260·

Skop, R. A. & Balasubramanian, S. 1997 A new twist on an old model for vortex-excited vibrations. *Journal of Fluids and Structures* **11,** 395–412.

Skop, R. A. & Griffin, O. M. 1975 On a theory for the vortex excited response of bluff cylinders. *Journal of Sound and Vibration* **41,** 263–274.

Stansby, P. K. 1976 The locking-on of vortex shedding due to the cross stream vibration of circular cylinders in uniform and shear flows. *Journal of Fluid Mechanics* **74,** 641–665.

Szewczyk, A. A., Balasubramanian, S., Haan, F. L. & Skop, R. A. 1997 Experiments on vortex-excited vibrations of pivoted circular cylinders. *Proceedings of the Fourth International Symposium on Fluid–Structure Interactions, Aeroelasticity, Flow-Induced Vibration and Noise* (eds M.P. Païdoussis *et al.*), AD-Vol. 53–1, pp. 177–184.

Thomson, W. T. 1988 *Theory of Vibrations with Applications.* Englewood Cliffs, NJ: Prentice-Hall.

Vandiver, J. K., Allen, D. & Li, L. 1996 The occurrence of lock-in under highly sheared conditions. *Journal of Fluids and Structures* **10,** 555–561.